SHOCK AND SHEAR INDUCED CHEMICAL REACTIONS IN Mo-Si, Nb-Si, AND Ti-Si SYSTEMS

M.A. Meyers[1], V.F. Nesterenko[1], K. S. Vecchio,[1] and S. S. Batsanov[2]
[1]University of California, La Jolla, CA 92093 USA
[2]National Institute of Standards, Mendeleevo, Moscow Region, Russia

ABSTRACT

Chemical reactions between metal (Mo, Nb, or Ti) and metalloid (Si) powder mixtures were produced by subjecting them to either shock compression or shock compression combined with high strain, high-strain-rate plastic deformation. It was confirmed that a threshold energy is required for the initiation of shock-induced chemical reactions. This threshold was originally proposed by Krueger and Vreeland[1] and corresponds to the energy required to melt a fraction of the silicon. The threshold energy is a function of the exothermicity of the reaction as well as porosity of the powder mixture. For a 35% porous mixture and powder size of 44 μm, the threshold values were 12 and 2 GPa for the synthesis of $MoSi_2$ and Ti_5Si_3, respectively. Under high strain, high-strain-rate deformation with superimposed pressures that are significantly below the threshold for shock initiation, chemical reaction can also be initiated at a sufficiently large plastic strain. Such is the case within shear bands, where the engineering shear strains can be as high as 50. For Nb-Si and Mo-Si mixtures, the reactions occurred only inside shear bands and for Ti-Si reactions initiated inside the bands and propagated throughout the entire specimen at a certain critical strain. Mechanisms for the initiation and propagation of shock- and shear-induced reaction are proposed.

Molybdenum and Molybdenum Alloys
Edited by A. Crowson, E.S. Chen, J.A. Shields,
and P.R. Subramanian
The Minerals, Metals & Materials Society, 1998

1. INTRODUCTION

Shock-induced reactions (or shock synthesis) have been studied since the 1960s but are still poorly understood, partly due to the fact that the reaction kinetics are very fast making experimental analysis of the reaction difficult. Shock-induced reactions are quite distinct from shock-induced phase transformations, such as the synthesis of diamond from graphite which is a diffusionless phase transformation. Shock-induced reactions also differ from detonations because only condensed phases are produced in the former, whereas the latter is characterized by gaseous products. Shock synthesis is closely related to combustion synthesis, and occurs in the same systems that undergo exothermic gasless combustion reactions. The thermite reaction ($Fe_2O_3 + 2Al \rightarrow 2Fe + Al_2O_3$) is prototypical of this class of reactions. The first report of these shock-induced reactions is due to Ryabinin *et al.* [2]. This initial discovery was followed by activity in Japan [3-5] and the USSR [6,7]. In the U.S., the pioneering work of Graham and co-workers [8-11] was followed by investigations by Vreeland and co-workers [1,12], Horie *et al.* [13,14]. Boslough [15], Thadhani and co-workers [16,17], and Yu *et al.* [18,19,20].

Shock synthesis of compounds from powders is triggered by the extraordinarily high energy deposition rate at the surfaces of the powders, thereby changing their configuration, forcing them in close contact, activating them by introducing large densities of defects, and heating them close to or even above their melting temperatures. Some fundamental questions regarding these reactions remain unanswered. Prominent among them are the following: (1) How can the extraordinarily high reaction rates encountered in shock compression be explained? (2) Are the phases formed under shock-synthesis conditions unique and non-equilibrium?

Another class of external stimulus responsible for initiating reactions is plastic shear. In quasi-static deformation,, Bridgman[20] discovered that shear strains superimposed on pressure was a powerful catalyst for chemical reactions. Under dynamic conditions, Lange and Ahrens [21] showed that the decomposition reaction of $CaCO_3$ into CO_2 and CaO was initiated by shear strains produced by parallel non-normal (inclined) impact. Yu [22] and Yu *et al.* [23] observed chemical reactions in regions of intense plastic deformation, in shock compression experiments. This led Nesterenko *et al.* [24] and Meyers *et al.* [25], to carry out explosive experiments on reactive powder mixtures at pressures below the threshold for shock-induced reaction. Chemical reactions were initiated in regions of intense plastic deformation.

In this paper shock-induced and shear-induced chemical reactions in the systems Mo-Si, Nb-Si and Ti-Si are presented and the mechanisms proposed earlier are reevaluated.

Ti-Si, Nb-Si and Mo-Si powder mixtures in their stoichiometric compositions of intermetallic compounds, Ti_5Si_3, $NbSi_2$ and $MoSi_2$ respectively, were used in this research. These compounds had been investigated in earlier shock experiments and therefore are good compositions for comparison. These systems have quite different enthalpies of reaction, ΔH :

$$\begin{aligned} 5Ti+3Si &\rightarrow Ti_5Si_3 \qquad \Delta H = -580 kJ/mole \\ Nb+2Si &\rightarrow NbSi_2 \qquad \Delta H = -138 kJ/mole \\ Mo+2Si &\rightarrow MoSi_2 \qquad \Delta H = -129.6 kJ/mole \end{aligned} \qquad (1)$$

These differences in heat of reaction can result in widely different sensitivities to the initiation and propagation of reaction. Meyers *et al.* [26] and Yu *et al.*[27] calculated threshold pressures for reaction at 65% initial density and obtained values of 1.5 GPa and 9 GPa for Ti_5Si_3 and $NbSi_2$, respectively. These calculations are based on the Krueger-Vreeland criterion [1,28] and are consistent with experimental results of Yu [27] and Vecchio *et al.* [29].

2.EXPERIMENTALPROCEDURES

Three elemental powder mixtures were used in this investigation: Nb-Si, Ti-Si and Mo-Si. The powders, produced by CERAC, had irregular shapes, and sizes smaller than 44μm (-325 mesh). The powders were mixed in the proportions to provide, upon reaction, the intermetallic compounds $NbSi_2$, Ti_5Si_3 and $MoSi_2$, for each system respectively. Three types of experimental setups were used: (a) planar impact ("Sawaoka" capsules); (b) cylindrical containers in the radial implosion mode; and (c) the thick-walled cylinder technique (also using a radial implosion mode).

2.1 Planar Impact (Sawaoka Setup)

Powders were encapsulated under controlled argon atmosphere in stainless steel capsules (internal dimensions of 15 mm diameter and 5 mm height). These capsules were subjected to shock compression in a Sawaoka fixture: this fixture is described in detail elsewhere [e.g. 29]: the system (cross-section) is shown in Fig. 1.

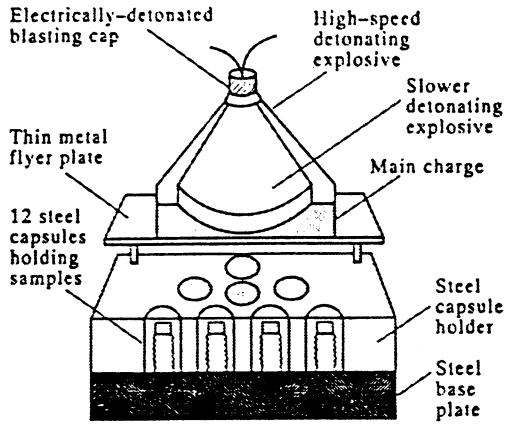

Figure 1: "Sawaoka" experimental set-up

Each system contains 12 capsules; four sectioned capsules are shown in Figure 1. A flyer plate is accelerated downwards by an explosive system consisting of a main charge (PBX 9404 explosive) initiated simultaneously along its top surface by an explosive lens consisting of two explosives with different detonation velocities. Impact velocities of 1.2 and 1.9 km/s were achieved by varying the quantity and type of explosive accelerating the flyer plate. Shock experiments were conducted on capsules at room temperature and others preheated to 773 K.

After shock processing, the specimen capsules were sectioned and analyzed by scanning and transmission electron microscopy. Since the shock experiment is very rapid, and the resultant thermal excursion short lived, the unreacted powder regions were considered chemically unchanged and subsequently used as pure elemental standards.

The pressure and temperatures induced by shock waves in the capsules were obtained from computer simulations, conducted by Norwood and Graham [30]. Two-dimensional effects are very important since the shock waves travel faster in the capsule than in the powder. Thus, the shock waves enter the capsules laterally, as well as at their top surface, generating highly inhomogeneous pressure and temperature regimes. This inhomogeneity in both pressures and temperatures was readily apparent within the recovered capsules, and was actually a highly useful effect since it enabled the analysis of unreacted, partially-reacted, and fully-reacted regions within the same specimen.

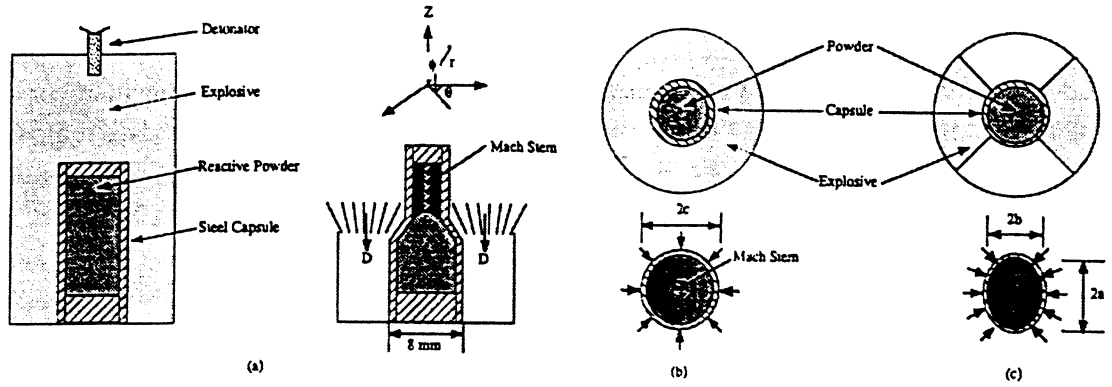

Figure 2: Symmetrical and asymmetrical collapse set-up

2.2 Co-axial (Symmetrical and Asymmetric Shock Wave Loading) Setup

The powders were mixed in the stoichometric proportions $NbSi_2$ and $MoSi_2$ and were loaded into tubular steel capsules. The powder mixture had an initial density of 70% of its theoretical value (30% porosity). These capsules, with external diameters of 14 mm and lengths of 70-80 mm, had walls with thickness of 2 mm (lower pressure experiments) and 3 mm (higher pressure experiments). The capsules were placed in explosive containers as shown in Fig. 2(a). The explosive was initiated at the top and the detonation wave traveled downwards, generating high pressures in the capsules. Details of the experimental setup are provided by Batsanov [31]. Three explosives were used with the characteristics: a high (ПВВ-4), a medium (RDX), and a low detonation velocity explosive (Ammonit). The Russian ПВВ-4 explosive is a plastic RDX-TNT mixture; RDX is used in powder form; the low detonation explosive, Ammonit, is an (ammonium nitrate)-(aromatic nitro compound) mixture. These explosives are intended at generating three pressure levels within the capsule. The cylindrical capsule geometry generates a pattern of converging shock waves in the powders, which is well described by Batsanov [32], Prummer [32], and Meyers and Wang [33], among others. The calculated pressures generated by the three explosives are 10.6 GPa (ПВВ-4), 6 GPa (RDX) and 2.8 GPa (Ammonit). It should be noted that these are only estimated values, and that the pressure is calculated neglecting the effect of the steel capsule. The actual pressures are probably somewhat lower. It is also important to note that the pressures are not constant throughout the cylinder cross-section. More accurate predictions, using hydrocode computation, have been developed by Reaugh [34].

Along the capsule axis, the convergent waves reinforce themselves and form a region in which the shock front is parallel to the propagation direction of detonation. This is the classical Mach stem, first observed in the propagation of shock waves in fluids. In the Mach stem, the shockwave velocity, U_s, equals the detonation velocity, D. From this equality, the pressure can be established. The pressures in the Mach stem are approximately seven times the pressure in the periphery. Only the ПВВ-4 explosive generated a pressure sufficiently high for Mach stem formation, and this Mach stem, shown schematically in Fig. 2(a,b), is clearly visible by observation of the polished cross-sections of the recovered specimens.

The use of an asymmetrical explosive loading, shown in Fig. 2(c), leads to a distortion of the capsule shape as well as the reduction in overall diameter due to densification. The macroscopic strains imparted by the three loading conditions can be calculated in the reference

system defined in Fig. 2(a). The length of the capsules remains unchanged, and therefore $\varepsilon_z = 0$. The macroscopic plastic strain corresponding to the porosity collapse is:

$$(1+\varepsilon_r)(1+\varepsilon_\theta)(1+\varepsilon_z) = 0.7$$
$$\varepsilon_r = \varepsilon_\theta = -0.16 \qquad (2)$$

The effective strain is $\varepsilon_{eff} = 0.2$. In the asymmetric capsules, an additional component of strain is present. It can be calculated from the dimensions a and b in Fig. 2(c). Assuming an elliptical distortion, the strain is given by:

$$\varepsilon_a = \ln(\frac{a}{c})$$
$$\varepsilon_b = \ln(\frac{b}{c})$$
$$\varepsilon_a = -\varepsilon_b = 0.55 \qquad (3)$$

The corresponding effective strain is $\varepsilon_{eff} = 0.64$. The specimens were observed by scanning electron microscopy. The backscattered electron imaging mode in all micrographs was used to differentiate the phases formed; the light phase is Mo or Nb, the dark phase is Si, and gray phases are compounds.

2.3 Thick-Walled Cylinder Technique

The thick-walled cylinder method was developed by Nesterenko *et al.* [35,36] for the investigation of high-strain, high-strain rate deformation of solid materials (such as metals, ceramics and polymers), and modified for the study of inert and reactive porous powder mixtures [37,38]; the schematic of the set-up is shown in Figure 3. Detonation is initiated at the top of the charge and propagates along the cylinder axis. The powder is first consolidated by a low amplitude explosive charge, which produces weak shock loading with pressures less than 1 GPa without any chemical reactions. An orifice is then drilled along the cylinder axis and a second explosive event is carried out. This second explosive produces significant plastic deformation in the densified powder layer. The velocity of the inner cylinder surface and the collapse time were measured by the noncontact electromagnetic method.

The experimental configurations were used to generate controlled and prescribed shear localization in porous samples. A porous powder was initially placed in a tubular cavity between a central copper rod and an outer copper tube. Explosive 1 (mixture of ammonite and sand in 3:1 volume ratio, with low detonation velocity was used to densify the powder. No significant shear localization was observed after this stage because the global deformation is sufficiently small. This stage produced mainly the densification of the powder. The following densifications were accomplished by the first explosive event (Figure 3a): Ti-Si mixture from ~35% to 65% of theoretical density; and Nb-Si mixture from ~*50%* to ~75% of theoretical density. A cylindrical hole with diameter 11 mm was drilled along the longitudinal axis of the copper rod and this composite cylinder was collapsed by the detonation of a second cylindrical explosive charge (ammonite, Figure 3b) with a detonation velocity of 4.0 km/sec, an initial density of 1 g/cm^3, and an outer diameter of 60 mm. This explosive event 2 produced significant plastic deformation in the densified porous layer which was highly localized in shear bands and not homogeneously distributed. To reduce and prescribe the global strains, a cylindrical copper

rod was inserted in the central orifice after explosive event 1. Shear initiator (metal glass) was used in some experiments (Figure 3c). This can provide the critical initiation and propagation conditions for shear localization and chemical reaction. Experiments with explosive event 3 of Ti-Si mixtures were also conducted without creating a central orifice. After this shock loading without collapse process, no shear localization or chemical reaction was observed. This confirms that the chemical reactions are truly strain controlled in the present experiments.

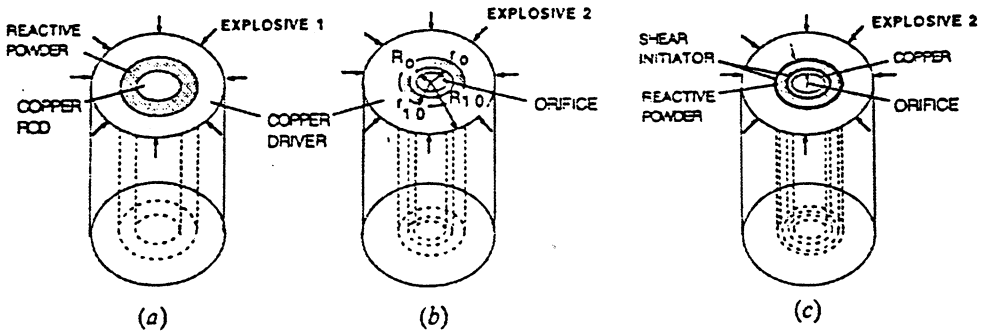

Figure 3: Thick-walled cylinder set-up

The global material strain can be obtained quantitatively from the strains in the incompressible copper shell driving the collapse process. The strain state in the uniformly deformed incompressible material is pure shear. The radial and tangential true strains for the copper shell, before the onset of localization, can be estimated by knowing the initial and final radii, r_i and r_f, at a general point:

$$\varepsilon_{rr} = -\varepsilon_{\varphi\varphi} = \ln\left(\frac{r_i}{r_f}\right) \tag{4}$$

The true strains in the inner and outer surfaces of the initial porous tubular layer can be found from Eqn. 4. The final radii r_f and R (or R_1) and initial radius R_0 (or R_{10}) (Figure 3) are experimentally measured and the value of r_i, which corresponds to a preselected value of r_f, can be calculated by using conservation of mass:

$$r_i^2 = r_f^2 + R_0^2 - R^2 = r_f^2 + R_{10}^2 - R_1^2 \tag{5}$$

where R and R_1 are the final radii of the inner hole and outer cylinder surface. The effective strains can be calculated according to the equation:

$$\varepsilon_{eff} = \frac{\sqrt{2}}{3}[(\varepsilon_{rr} - \varepsilon_{\varphi\varphi})^2 + (\varepsilon_{\varphi\varphi} - \varepsilon_{zz})^2 + (\varepsilon_{zz} - \varepsilon_{rr})^2]^{1/2} = \frac{2}{\sqrt{3}}\varepsilon_{rr} \tag{6}$$

The global strains in copper at the boundary with the porous layer outside the shear localization region can be estimated by using Eqns. 4 and 6. The state of stress of these plane strain experiments is very difficult to control because during plastic flow it is determined by the material's strength and its dependence on temperature, strain, and strain rate. The following two main features of this method should be mentioned:

(i) The weak shock waves propagating in materials in the first stage or collapse (explosive event 1) have no noticeable influence on the chemical reaction; their amplitudes are less than 1 GPa.

(ii) The superimposed "hydrostatic" pressure inside collapsing incompressible cylinder, as a result of its acceleration toward the center, is less than 0.1 GPa.

Thus, pressure effects can be neglected to a first approximation and chemical processes are mainly strain controlled.

3. EXPERIMENTAL RESULTS AND DISCUSSION

3.1 Shock-Induced Chemical Reactions

3.1.1 Sawaoka Capsules

Figure 4 shows reaction maps of the cross-sections for the recovered capsules for the Nb-Si and Mo-Si samples; fully-reacted, partially-reacted, and unreacted regions are evident. Upon recovery, the specimens were considerably cracked, and portions of the specimens were lost during sectioning.

Backscattered electron micrographs of a polished section of the Mo-Si sample shocked at room temperature and low velocity (1.2 km/s) are shown in Fig.5. Analysis of the other two Mo-Si samples will not be presented here, but examination of these samples revealed structures similar to the corresponding Nb-Si samples. Figure 5 shows the partially-reacted region which made up the majority of the sample and consisted of Mo particles surrounded by a reaction layer of $MoSi_2$ nodules and embedded within a two-phase matrix of $MoSi_2$ nodules and silicon. In many instances, the entire Mo particle has been reacted to form the $MoSi_2$ phase, as indicated by an arrow in Fig 5(a). Figure 5(b) shows the transition region from the partially-reacted to fully-reacted material located near the bottom of the capsule. No additional interfacial reaction product could be observed in this sample, unlike the Nb-Si samples. In the unreacted region, the Mo particles appear to fragment along grain boundaries within the particles, while the silicon particles seem to have undergone intense plastic deformation.

The fully-reacted regions for the Nb-Si and Mo-Si samples were essentially identical in terms of macroscopic morphology. Voids were present throughout, resulting from either solidification shrinkage, gases evolved during the reaction, or tensile stresses imposed on the compact prior to solidification. The presence of spherical voids, as well as dendritic structures observed are evidence of melting and re-solidification.

3.1.2 Co-axial Symmetrical Configuration

These experiments were conducted using explosive ПВВ-4, with a detonation velocity of 7.4 km s^{-1}. Both the Mo + 2Si and Nb + 2Si systems exhibited unreacted, partially reacted, and fully reacted regions, Fig 6. There is a clear boundary between them, and the central Mach stem corresponds to the fully reacted region. The unreacted and partially reacted regions are seen Fig. 6(a) (Mo + 2Si). The unreacted region corresponds to the periphery of the circular section and was subjected to a calculated pressure of 10 GPa. There is no evidence of Si melting or reaction. Vecchio et al. [29] observed the onset of reaction in shock-compressed Nb + 2Si and Mo + 2Si powder mixtures with the same initial porosity as the present investigation: the onset for reaction was 7-12 GPa. The partially reacted region is characterized by the formation of $NbSi_2$ and $MoSi_2$ spherules, as observed first by Yu and Meyers [18] and described in detail by Vecchio *et al.* [29] and Meyers *et al.* [26]. These spherules have diameters of 0.5-2.0 μm and are larger in the periphery of Mo particles, as seen in Fig. 6(b). As the Mo particles are consumed,

the diameters of the spherules decrease. The gradation of spherule size is seen in the totally consumed particles of Fig. 7(a). Closer to the cylinder axis, a fully reacted region is observed.

The presence of profuse spheroidal voids is an indication of complete melting of the reaction products. Two phases are seen for the Nb + 2Si system. These are probably $NbSi_2$ and Nb_3Si_3. These particles become gradually more faceted. Their maximum size is approximately 10 μm. For Mo-Si system Vecchio *et al.* [29] identified the product of complete reaction as Mo_5Si_3. The detailed nature of reaction, "frozen in" the partially reacted region, can be seen in Fig 6(a,b).

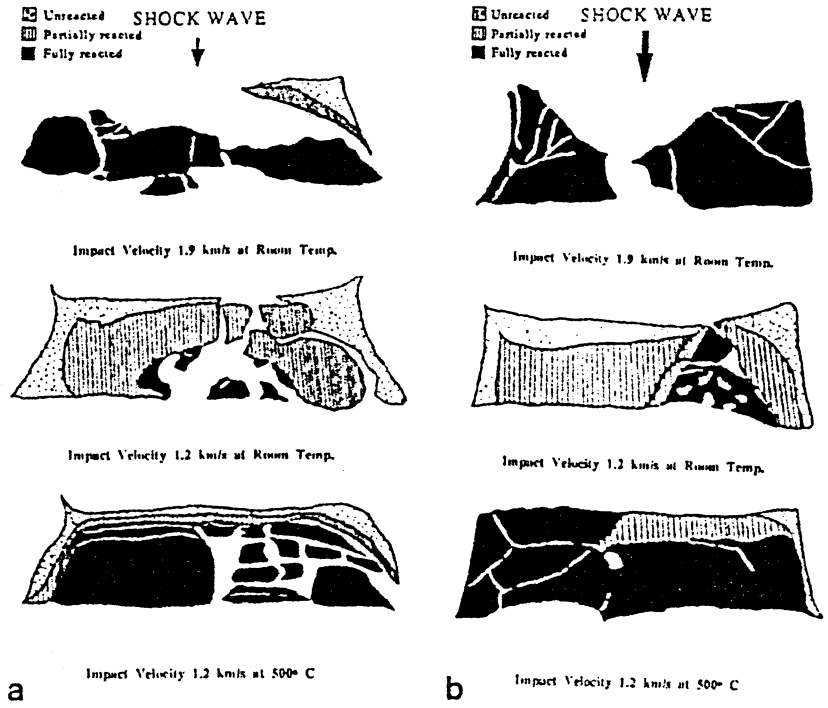

Figure 4: Cross-sections of Sawaoka capsules with (a) Nb+Si and (b) Mo+Si subjected to different shock compression pulses.

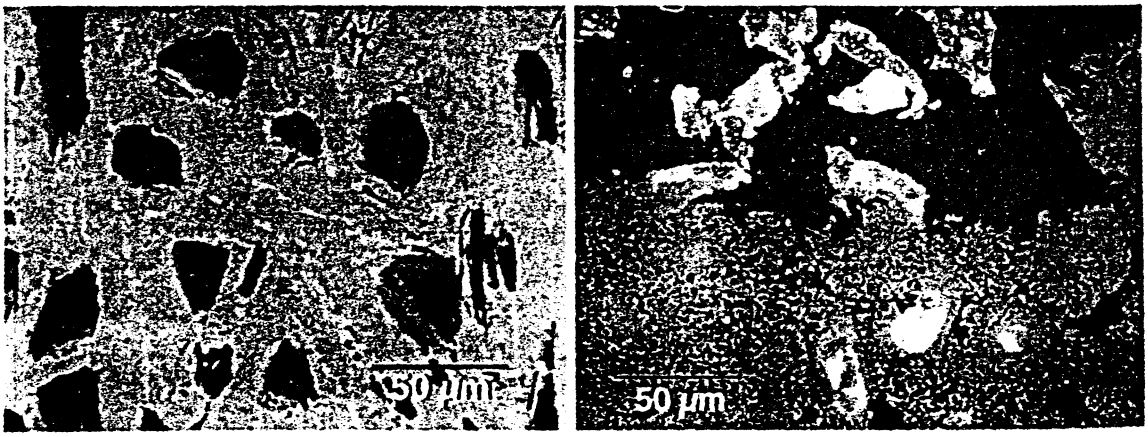

(a) (b)

Figure 5: (a) Fully reacted region and (b) Boundary between unreacted and partially reacted regions in Mo+Si mixture for Sawaoka capsule.

It is very significant that a sharp interface between (mostly) unreacted and partially reacted regions exists. There has been considerable debate over the time at which the shock-induced chemical reactions occur. From Fig. 6(a) it is evident that the reaction was triggered by the shock wave, and not by post-shock thermal effects. The physical state of reactants has been analyzed by Vecchio *et al.* [29] and Meyers *et al.* [26]. They proposed that silicon melts, whereas niobium (or molybdenum) remains in the solid state. Thadhani [39] recently carried out a systematic analysis of chemical reactions produced by shock compression, classifying them into shock-induced (reaching completion during shock-wave passage) and shock-assisted (occurring primarily after shock compression). From the present results, it is not possible to establish clearly which of these processes is taking place. If thermal (post shock) effects were dominant, one would observe a gradual reduction in the extent of reaction with distance from the interface. Such is clearly not the case; Fig. 6(b) shows details of the reaction for both the Nb+2Si and Mo+2Si cases. The reaction proceeds according to mechanism described in Section 3.1.3. Fig. 7 shows details of the separation of the $NbSi_2$ solidifies, stresses are set up which lead to the separation of the spherules from the Nb substrate. The spherules subsequently move into the Si, which is molten during reaction. The melting points of the three phases are: Si_{mp}= 1685 K; Nb_{mp}= 2740 K; $NbSi_{2mp}$= 2420 K. The same mechanism is seen to operate for $MoSi_2$.

3.1.3 Proposed Reaction Mechanism

The analysis of the partially-reacted regions in the Nb-Si and Mo-Si shock experiments revealed the detailed nature of the reaction sequence and mechanisms (for the sake of brevity only the Nb-Si system will be discussed below, however this analysis applies equally well to the Mo-Si system). Reaction mechanism proposed below is given by Meyers *et al.*[26]. The preponderance of small $NbSi_2$ particles surrounded by silicon, as well as the existence of $NbSi_2$ particles attached to the niobium particles (Figs. 5 and 6) are evidence for a reaction mechanism in which the $NbSi_2$ or $MoSi_2$ particles are continuously being generated at the interface and ejected into the (molten) silicon. This is shown in the sequence displayed in Fig. 7. Thus, no permanent diffusion barrier that would slow down the reaction process is formed, and reaction can proceed at a constant rate until the entire metal (Nb or Mo) or silicon is consumed. The shock-induced reaction is initiated along the solid metal-molten Si interface. After reaction has proceeded to a certain extent, surface (interfacial) forces become dominant, and the liquid reaction product agglomerates, forming a spherule. At this point, reaction kinetics are drastically decreased, due to the reduction in the Nb-Si interfacial area, and solidification of the disilicide sphere starts. As the sphere solidifies, new nuclei form along the Nb-Si interface. The new nuclei grow, agglomerate into spheres when they reach a critical size, and thereby form neighboring spheres. As these neighboring spheres solidify, they exert forces on the first sphere, expelling it into the molten silicon, and thus exposing fresh surfaces. This reaction process can continue unimpeded, until the reactants are consumed. In addition, turbulent flow of the liquid silicon under shock can also contribute to the detachment of the spherules from the interface.

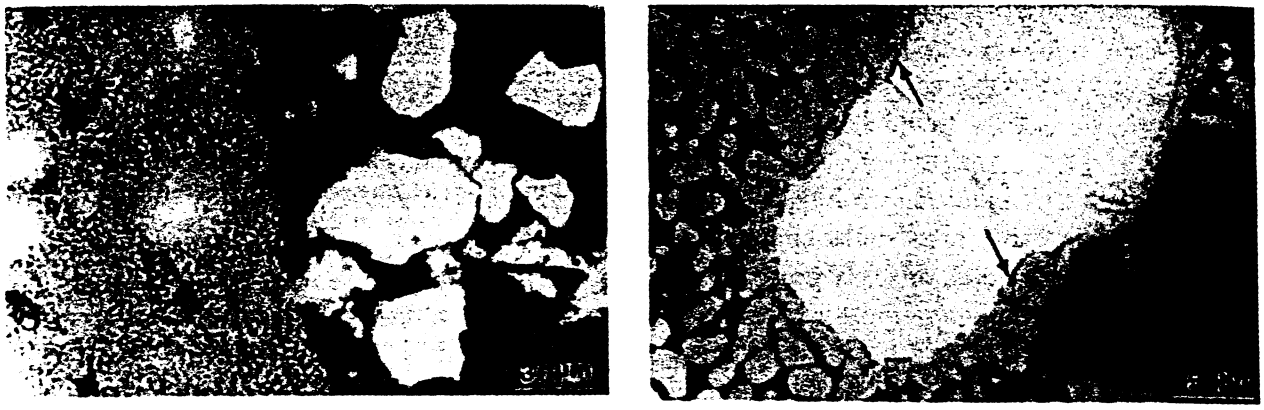

Figure 6: (a) Interface between reacted and partially reacted regions in co-axial symmetrical collapse geometry; (b) higher magnification view of Mo particle surrounded by $MoSi_2$ spherules.

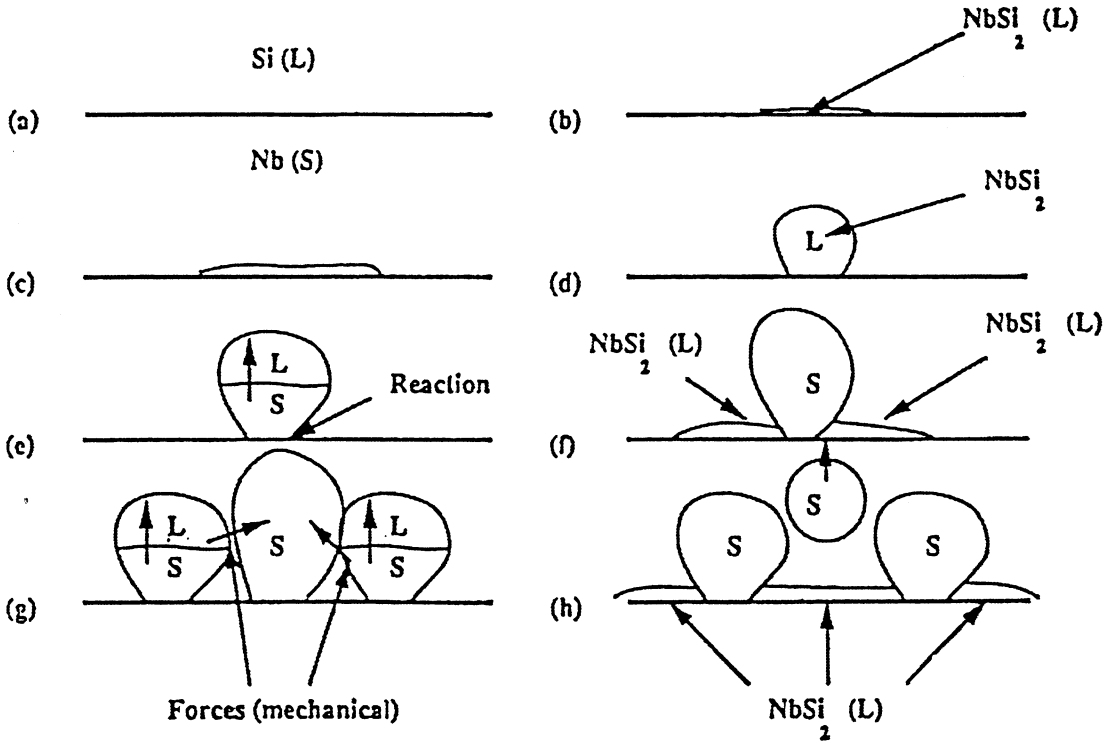

Figure 7: Sequence of events leading to the formation and ejection of $NbSi_2$ (or $MoSi_2$) spherules (after Vecchio *et al.* [29]).

3.2 Shear-Induced Chemical Reaction

3.2.1 Asymmetrical Configurations

Experiments were conducted at two detonation velocities, 4.4 and 6.2 km s^{-1}, yielding pressures of approximately 2.8 and 6 GPa. These pressure levels are below the critical level for shock induced chemical reactions, defined by Krueger *et al.* [1] and determined for Nb and Mo

silicides by Vecchio *et al.* [29]. The effective strain accomplished through asymmetric loading is 0.64. The deformation energy per unit mass can be estimated from the simple expression:

$$E_d = \frac{\sigma_{eff}\varepsilon_{eff}}{\rho} \tag{7}$$

where σ_{eff} is the flow stress of the material under the imposed conditions and ρ is the density. It is possible to estimate the flow stress of the densified Nb-Si or Mo-Si mixture from a constitutive equation, such as the Johnson-Cook equation [41]

$$\sigma = (\sigma_0 + B\varepsilon^{n})\left(1 + C\log\frac{\dot{\varepsilon}}{\dot{\varepsilon}_0}\right)\left(1 + \frac{T^*}{T_m^*}\right)^m \tag{8}$$

σ_0, B, C, m and n are parameters and T^* and T_m^* are normalized reference and melting temperatures. Ignoring work hardening and thermal softening, Eq. 8 is reduced to:

$$\sigma = \sigma_0\left(1 + C\log\frac{\dot{\varepsilon}}{\dot{\varepsilon}_0}\right) \tag{9}$$

It is possible to estimate the strain rate from the collapse velocity of the capsule containing the powder. It has been estimated to be equal to 800 m s^{-1}, by Ferreira *et al.* [40]. Thus, the strain rate is ($2r$ is the diameter of the capsule):

$$\dot{\varepsilon} = \frac{v}{2r} = \frac{800}{10\times10^{-3}} \cong 0.8\times10^5\, s^{-1} \tag{10}$$

The compressive strength of Nb, under quasi-static conditions, is ≈300 MPa: for Si, it is estimated to be 90 MPa. The value of C, the strain-rate sensitivity, can be estimated from data collected by Johnson and Cook [41]. From an average value for a number of materials ($C=1$), and applying Eq. 9, the flow stress can be estimated as:

$$\sigma_{eff} = 800 \text{ MPa}$$

The application of Eq. 7 leads to the estimate of the deformation energy ($\rho \cong 4.3\times10^3\, kg\cdot m^{-3}$)

$$E_d = 120 Jg^{-1}$$

This value is quite low in comparison with the shock energy in experiments by Meyers *et al.* [26] to initiate the reaction based on experimental observations: 700-1200 J g^{-1}. The Krueger-Vreeland threshold energy expression has the form:

$$E_{th} = E_s = \frac{1}{2}P(V_{00} - V) \tag{11}$$

where E_{th} and E_s are the threshold and shock energies (equal), P is the shock pressure, and V_{00} and V are the initial and shock specific volume respectively. The Krueger-Vreeland threshold energy includes, at the micro-mechanical level, the energy necessary to collapse the voids (geometrically-necessary plastic deformation), microkinetic energy (proposed by Nesterenko [43]) and a frictional energy. The various energetic terms are described by Meyers *et al.*[26]. The microkinetic energy represents, to a first approximation, the difference between the P-V triangle and the "quasi-static" densification energy, which is reasonably well represented by the Carroll-Holt expression. Yu *et al.* [23] proposed a modified expression for the minimum energy

which incorporates the plastic deformation energy. The total energy is the sum of the shock energy (which incorporates plastic deformation) and the deformation energy, E_d, due to non-shock processes:

$$E_t = E_s + E_d = \frac{1}{2}P(V_{00} - V) + \left(1 + C\log\frac{\dot{\varepsilon}}{\dot{\varepsilon}_0}\right)\sigma_{eff} \qquad (12)$$

The condition for initiation is, then:

$$E_t \geq E_{th}$$

The asymmetric experiments yielded shock energies (Eq. 11) of 190 Jg^{-1} and 300 Jg^{-1} for ammonit and RDX, respectively; the energy due to macroscopic plastic deformation (120 J g^{-1}). Applying Eq.12:

$$(E_t)_{ammonit} = 310 Jg^{-1}$$

$$(E_t)_{RDX} = 420 Jg^{-1}$$

These values are still insufficient to initiate the reaction.

Localization of plastic deformation in narrow shear bands was observed in the system shock compressed with RDX (detonation velocity of 6.2 km s^{-1} and pressure of 6 GPa). Within the shear localization region high plastic strains are set up. Fig. 8 shows one such area for Mo + 2Si. The shear-band areas are characterized by fracturing of the Mo particles. The energy of deformation. for a shear strain of 10, ignoring thermal softening, is equal to 1000 Jg^{-1}. This value is of the same order of magnitude as the threshold energy and can indeed be sufficient to trigger the reaction. Indeed, selected areas within the shear localization regions exhibited clear evidence of reaction. The reacted areas are marked by arrows A in Fig. 8. The deformed Mo particles and flaky splinters, produced by the intense plastic deformation, are surrounded by reacted material. The mechanism for reaction seems to be analogous as that under shock compression, but the diameter of the spherules is considerably smaller: 0.1-0.4 μm as seen in Fig. 8. The silicon in Fig. 8 shows spheroidal voids (marked by arrow B) and this is strongly suggestive of melting and resolidification. Nesterenko *et al.* [37,38] propose a specific mechanism for shear-induced reaction involving vorticity, partial fracture and melting.

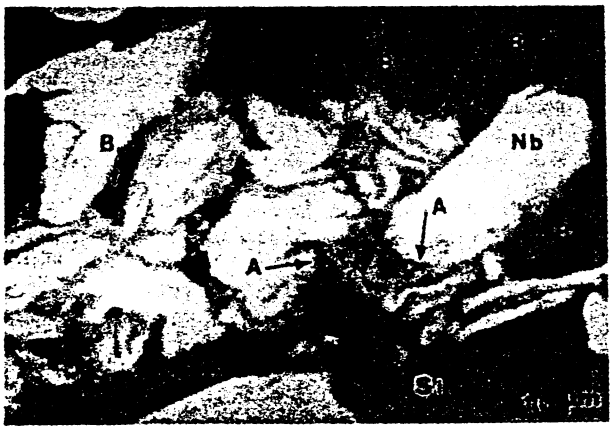

Figure 8: Partial reaction within region of intense localized shear in co-axial asymmetric collapse geometry; regions 'A' mark reaction products.

3.2.3 Reaction Inside Strain-Controlled Shear Bands

It has recently been observed and carefully analyzed, using the thick-walled cylinder technique that plastic deformation without shock-wave loading can initiate chemical reactions in powder mixtures. This occurs in regions of high localized plastic strains and under high-strain-rate deformation which ensures adiabatic or quasi-adiabatic conditions in the narrow deformation bands. This region is intermediary thermal combustion synthesis and shock-induced reactions. The associated temperature rise and mechanical flow of constituents are sufficient to initiate the chemical reaction with these regions. Research carried out by Chen et al.[38] and Nesterenko et al.[42]: (a) established the critical conditions for initiation and propagation of reactions in two systems with widely varying heats of reaction: Nb-Si (ΔH = -138 kJ/mole) and Ti-Si (-580 kJ/mole) and (b) modeled the initiation of reaction and its propagation throughout the inter-shear band regions and explain on this basis difference between these two systems. Fig. 9 shows the cross-sections of Ti-Si samples after explosive event 2. Shear localization is a prominent feature of the plastic deformation process. The shear band spacing L, is unaffected by the scale of experiments for the Nb-Si mixtures. The spacing of the shear bands for Nb-Si mixture is approximately the same as for the Ti-Si mixture: 600-1000 μm.

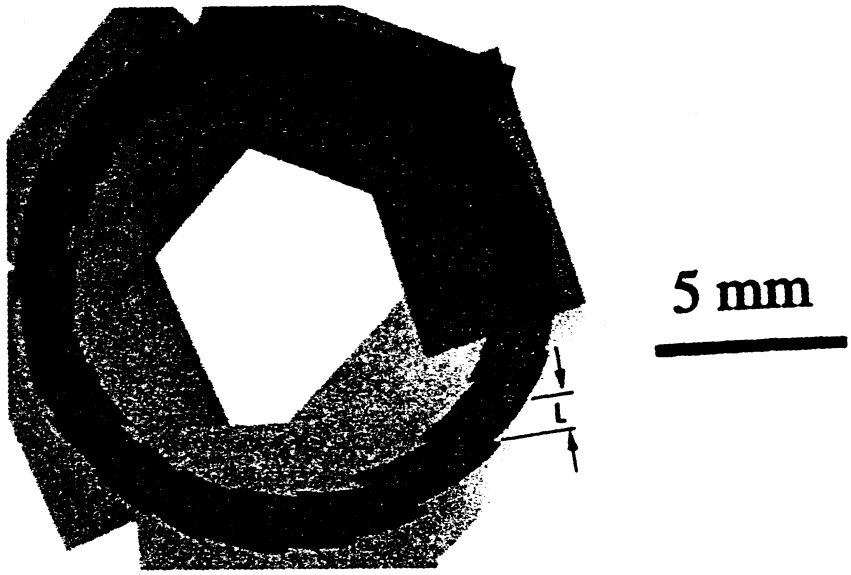

Figure 9: Shear localization, evidenced by steps in Ti+Si mixture subjected to deformation in thick-walled cylinder

Shear-initiated chemical reactions are observed in the shear localization regions in both Ti-Si, and Nb-Si mixtures (Figure 10). The shear deformation work can lead to the reaction ignition inside shear band and propagation of the reaction throughout the material. Since the strain rate is high, there is not sufficient time for the heat resulting from shear deformation to be conducted away from the shear localization regions. Therefore, the temperature in the shear localization regions increases to very high values. This localized temperature zone is a heat source. The shear localization regions can be treated as one-dimensional array of "hot spots" where chemical reactions are possible. Once the temperature reaches some critical value, the chemical reactions are initiated. Calculations of heat evolution for an idealized periodic distribution of "hot spots" in reactive powder mixtures were carried out. Figure 11(a) is a schematic illustration of the idealized model. The "hot" shear localization regions (shaded areas)

have a width, d, and a spacing, L. The temperature inside the shear localization regions increases to T_s during deformation (shown in top of Fig. 11(a)). If T_s is sufficiently high, the chemical reactions between reactive powder mixtures are initiated. At this time, the reaction heat is released and the temperature increases by some amount, ΔT; the temperature inside the shear localization regions becomes $T_s + \Delta T$ (bottom part at Fig. 11(b)). However, the surrounding powder mixtures are at a lower temperature ($T = T_0$). The heat will be conducted to the surrounding material. The conservation of energy for this model is given by:

$$\rho C_p \frac{\partial T}{\partial t} = k \frac{\partial^2 T}{\partial x^2} + \rho Q \frac{\partial \eta}{\partial t} + \tau \frac{\partial \gamma}{\partial t} \qquad (13)$$

where ρ is the density (kg/m^3), C_p is the heat capacity (J/kg K), k is the thermal conductivity (W/m K), η is the degree of conversion, τ is the shear stress (N/m^2), γ is the shear strain.

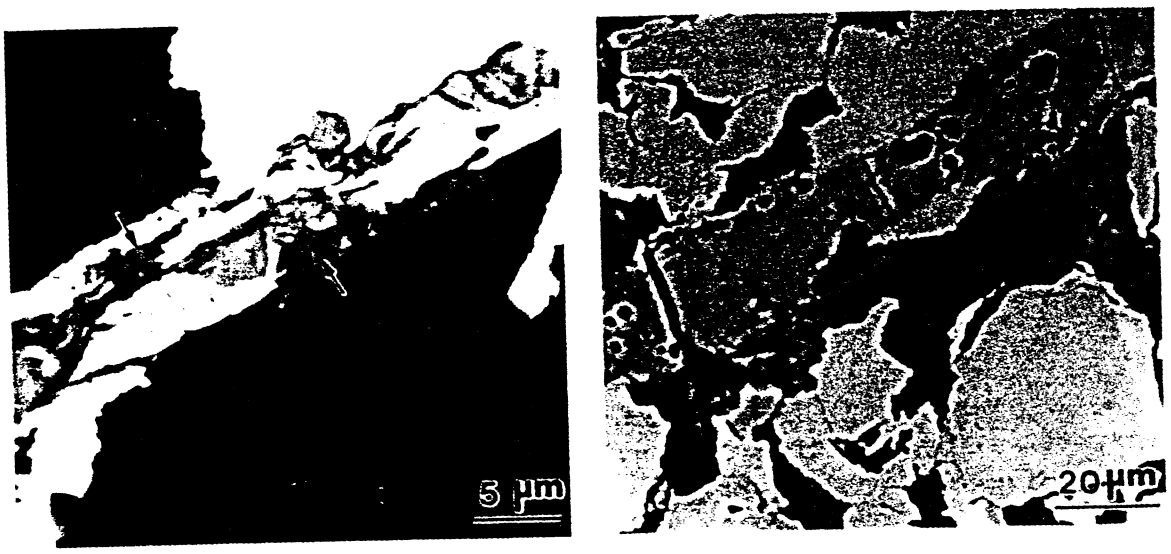

Figure 10: Shear localization in Ti+Si mixture: (a) partial reaction at $\varepsilon_{eff} = 0.33$, (b) full reaction at $\varepsilon_{eff} = 0.35$.

For the sake of simplicity, the following assumptions are made:

(a) The shear localization and the chemical reaction do not occur simultaneously, i.e. they occur sequentially.

(b) Define t = 0 when T_s is reached. After this moment the term representing deformation work can be eliminated because at high values of T_s the drop in material strength makes this term negligible in comparison with heat release due to the reaction. Equation 11 can be rewritten as following:

$$\rho C_p \frac{\partial T}{\partial t} = k \frac{\partial^2 T}{\partial x^2} \qquad (14)$$

The Arrhenius equation is used for reaction kinetics:

$$\frac{\partial \eta}{\partial t} = K_i (1-\eta) \exp(-E / RT) \qquad (15)$$

In Eq. 15, the rate constant K_i can be greatly different inside and outside shear band. The intensive particle fracture, vorticity and relative motion of components can greatly intensify yield of reaction.

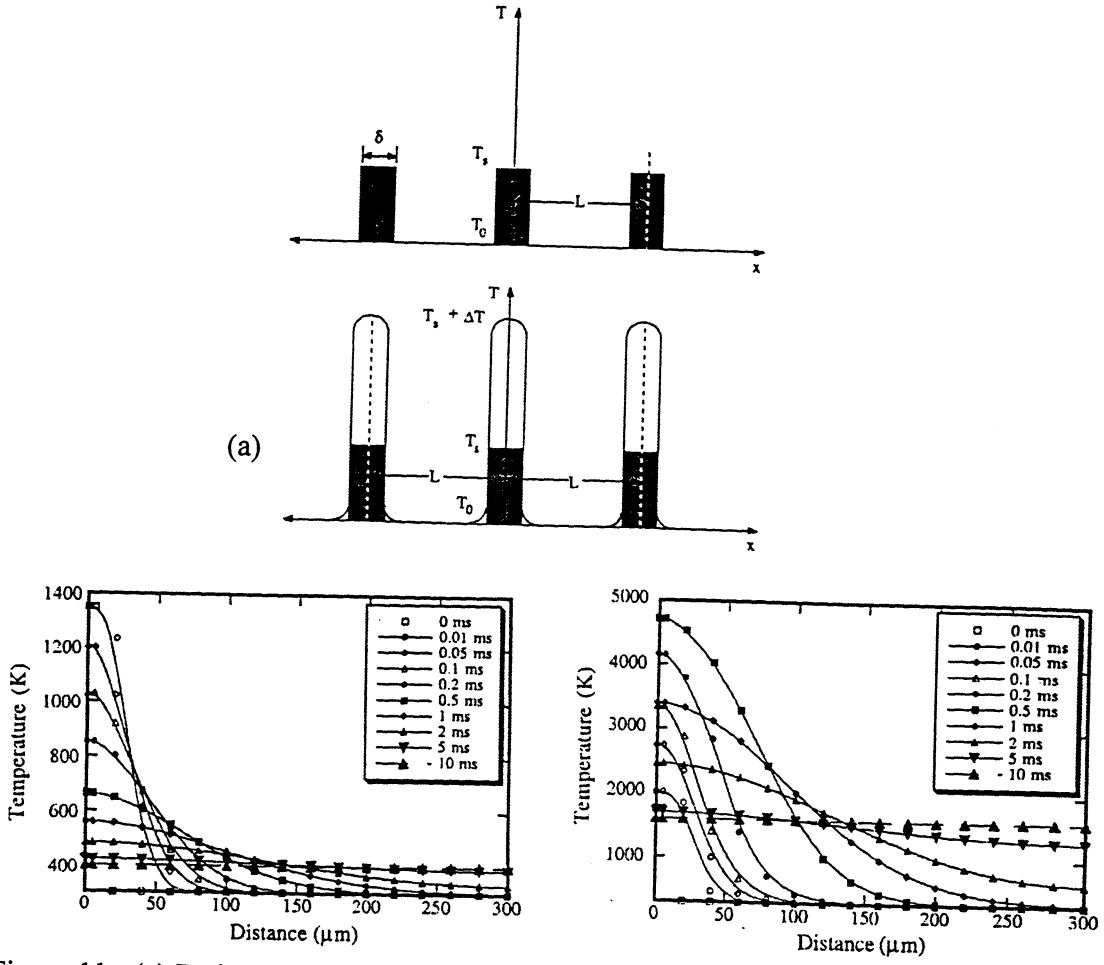

Figure 11: (a) Periodic 'hot spots' pattern, (b) Calculated temperature profiles for Ti+Si: temperatures of T_s = 1350 K (left) and 1750 K (right)

This reaction kinetics is common in the combustion synthesis literature. One of the problems connected with this type of kinetics is that it theoretically provides possibility for complete reaction at any temperature under thermal isolation. Nevertheless for self propagating mode of combustion synthesis these kinetics allow identification of some critical conditions like ignition temperature which defined as the minimum temperature required to initiate a self-propagating reaction wave with stationary profile under specified boundary conditions. This ignition temperature is a function of thermophysical parameters of reactive material and boundary conditions. In another case, simultaneous combustion mode of reaction, the heating of an entire sample at a constant rate can result in bulk combustion at some critical temperature which is also called ignition temperature. This ignition temperature is also a function of material properties like density and boundary conditions. In a conservative approach, the ignition temperature can be associated with the melting temperature of one of the component, in our case with melting of Si. In some cases, the ignition temperature can be essentially less than the melting temperature of components as a result of enhanced solid state reactivity of powders after plastic deformation. In the problem of reaction initiation by shear bands, the achievement of the steady combustion wave propagation regime can not be considered as the necessary

condition. It is considered that the condition of ignition is fulfilled if the quasi-equilibrium temperature in the unit cell (after fast stage of heat propagation from shear band and subsequent partial reaction) is close to the melting temperature of Si. It is supposed that the final stage of reaction can be accomplished in the simultaneous combustion mode under natural boundary conditions provided by the contact of reactive material with copper.
Initial conditions are:

$$T(x,0) = \begin{cases} T_s \\ T_0 \end{cases} \quad at \quad \begin{matrix} 0 \le x < \delta/2, \;\; L-\delta/2 < x \le L \\ \delta/2 \le x \le L-\delta/2 \end{matrix} \tag{16}$$

The boundary conditions represent zero heat flux at points of symmetry in l-D system of "hot" layers (Fig.11b):

$$\frac{\partial\, T(x,t)}{\partial\, x} = 0 \quad at \quad x = 0, L/2, L \tag{17}$$

In real experiments, the reactive mixture is encapsulated into a cold copper jacket (Fig. 3) which determines macroscopic boundary condition on the interface of reactive mixture and copper. In accordance with experiments, the condition of ignition is determined as achievement of the intermediate temperature, the melting temperature of Si in the thermoisolated unit cell. It means that if $T_{m,Si}$ is reached, then the rate of subsequent reaction will be fast enough to complete reaction in the bulk, except within a thin layer adjacent to the copper.
Thermophysical properties are assumed constant and equal: $\rho = 3.85 \times 10^3$ kg/m^3, C_p=*570* J/kg K, k = *36.5 W/mK*, E=*125* kJ/mol and Q = 1792 J/kg. The reaction rate outside shear band K_0 was estimated by Chen *et al.* [42] ($K_0 = 2.6 \times 10^5$ s^{-1}) and applied to estimate the temperature profile at different times.

The calculated temperature profiles for Ti-Si system at T_s= 1350 K (γ=10), and 1750 K (γ = 60) [42], are shown in Fig. 11(b). The calculated temperature profiles can be used to predict the critical parameters for initiation and propagation of the reaction. For example, if the final equilibrium temperature is still lower, but close to the initiation temperature $T_{m,Si}$ it is probable that conditions are close to the threshold for the complete reaction in the material bulk. Slight increase of the initial temperature T_s or shear strain γ will result in complete reaction.

At T_s =1350 K, heat transfer dominant and there is no temperature increase inside the shear band as shown in Fig. 11(top) due to the absence of chemical reaction.

When temperature at initial moment reaches 1750 K, the reaction rate is comparably higher than at $T_s \approx 1350K$. Therefore, the heat can be sustained inside the shear band and temperature experiences a dramatic increase. After reaction completion inside the shear band, the temperature inside the shear band begins to decrease and the temperature outside the shear band increases due to heat conduction. As the temperature in some point outside the shear band reaches a critical value $T_{m,Si}$, the reaction can be initiated. The reaction eventually propagates through the entire specimen. The equilibrium temperature in this case, shown in Fig. 11(b)(bottom), is ~1600 K. Experimental results show that the entire specimen was fully reacted. Therefore the assumption that the ignition temperature for reaction $5Ti+3Si \rightarrow Ti_5Si_3$ is close to the melting point of Si (1685 K) in conditions of current experiments is reasonable. It should be mentioned that change of reaction kinetics does not result in the change of heat release if reaction is completed. The tenfold increase of K inside shear band did not result in an essential change of temperature profiles outside shear band areas because the thickness of the shear band $\delta << L$ and initial conditions provide great difference in reaction yield inside ("hot" area) and outside shear band ("cold" area) at initial stage of the process even at the same K [42].

Shear-initiated chemical reactions are also observed in the shear localization regions in Nb-Si mixtures. However, the reaction cannot propagate through the entire specimen under the same strain condition. Using the "hot spot" model, one can estimate the temperature distribution at different times. The required parameters and thermal properties for this model in Nb-Si system are: initial temperature inside shear band T_s = 2000 K - 2300 K (corresponding to γ =20 - 60), T_0 = 300 K outside shear band. Density ρ = 4.2 g/cm^3; heat capacity C_p=540 J/kg K; thermal conductivity, k=16.8 *W/m* K and heat release from reaction, Q= 926 J/kg. The reaction kinetics was described by the same Arrhenius equation. In contrast with the Ti-Si system, the reaction propagates outside of the shear localization area at the distances comparable to the shear band thickness and is rapidly quenched with "equilibrium" temperature being much lower than Si melting temperature. This result is in accord with the experimental observations[42].

4. CONCLUSIONS

The three classes of explosive experiments are complementary and produced results that considerably increase our understanding of chemical reactions under high-strain-rate loading conditions.

4.1 Planar Impact (Sawaoka Setup)

It was possible to successfully initiate and propagate shock-induced reactions for the two systems investigated (Nb-Si and Mo-Si), and the extent of reaction was found to increase with shock energy, shock temperature, and the energy of reaction.

The following qualitative statements can be made: (a) as the heat of reaction increases, the shock pressure/temperature necessary for full reaction decreases, and (b) the extent of shock-induced reaction increases with shock energy, at a constant temperature, and with temperature, at a constant shock energy.

Electron microscopy observations reveal that the main reaction product in the partially-reacted regions is the disilicide formed from the molten state as spherules with radii of approximately 1-2 μm. These spherules are formed at the metal-Si interface and are expelled into the silicon. There is clear indication that silicon melting is a prerequisite for shock-induced reactions.

The kinetics in static solid-state reaction were established and found to be lower, by ~10^8 compared to the kinetics in shock compression. A reaction mechanism under shock compression for the metal-Si interface is proposed involving the dissolution of Nb or Mo into molten Si, producing the molten intermetallic, with its subsequent spheroidization, solidification, and expulsion into the surrounding liquid silicon melt. In this reaction mechanism fresh solid-liquid interface is continuously maintained, enabling a high reaction rate.

4.2 Coaxial Symmetrical Experiments

Shock compression of Nb-Si and Mo-Si elemental powder mixtures in cylindrical capsules(using an explosive with detonation velocity of 7.4 km s^{-1}) yielded two regimes of pressure: a central Mach stem with a pressure of $\approx$ 70 GPa, and a peripheral area with P $\approx$ 10 GPa. The pressure was sufficient to produce full reaction with complete melting. Although the experiments do not directly establish whether the reaction is shock-assisted or shock-induced (completion after and during shock process, respectively) the sharp reacted - unreacted interface strongly suggests a shock-induced reaction; the peripheral region did not exhibit reaction. At the

boundary between the two regions, a partially reacted region was observed, and the mechanism of reaction was by the formation of a liquid reacted Nb-Si or Mo-Si layer surrounding the solid Nb and Mo particles, respectively; this was followed by their spheroidization by interfacial energy minimization, solidification, and detachment from the interface. The mechanism is the same as that proposed by Meyers *et al.*[26] and Vecchio *et al.* [29].

4.3 Thick-Walled Cylinder Experiments

For shear-induced chemical reactions, at shock pressures below the threshold for shock-induced reactions, the following conclusion were reached.

Localized reactive shear bands in Ti-Si and Nb-Si mixtures were generated. In some experiments, reactions propagated through the entire specimen at critical strain in Ti-Si system; however, they could not take place in the Nb-Si system, under the same imposed conditions. Shear-band spacing is independent of the scale of experiment; for assemblies with mean diameters of 18 mm and 34 mm, the shear-band spacing is the same: L ~ 0.6-1 mm. Heat transfer coupled with chemical reaction calculations with periodic boundary conditions are used to evaluate the evolution of the temperature history from shear initiation to thermal equilibrium. The model predicts, correctly, the propagation of reaction into the inter-shear spaces for Ti-Si, at the experimentally observed values of shear strain in shear bands; it also predicts extinction of the reaction in the vicinity of the shear bands for the Nb-Si, in agreement with observed results. From the advance of the reaction front for the Ti-Si mixture, parallel to the shear-band interface, it is possible to estimate a reaction time, by integrating the velocity (variable) over the shear-band semi-spacing. The reaction time is estimated to be, for Ti-Si, 10 ms and does not depend on the sample size being function of the shear band spacing. This is in stark contrast with combustion synthesis, where the reaction time depends on the sample size, and shock compression synthesis, where the reaction time can be as low as 1 μs. Thus, an intermediate reaction regime has been obtained. Reaction rate inside shear band can be optimized for maximum reaction yield.

5. ACKNOWLEDGMENTS

This research was supported by the U.S. Army Research Office contract DAAH 04-93-6-0261, Office of Naval Research Contract N00014-94-1-1040(Program officer Dr. J. Goldwasser) and by the U.S. Army Research Office under contract MURI DAAH04-96-1-0376.

6. REFERENCES

1. B. Krueger and T. Vreeland Jr, in Shock-Wave and High-Strain-Rate Phenomena in Materials (New York, NY: Marcel Dekker, Inc., 1992), 241.
2. Yu. N. Ryabinin, Soviet Phys. Tech., Phys., 1(1956) 2575
3. Y. Nomura, Kagaku Kogyu, 16(1963) 123
4. Y.Nomura, J. Less-Common Metals, 11(1966) 378
5. Y. Horiguchi, J. Am. Ceram. Soc., 49(1966) 519
6. G.A. Adadurov et al., Polymer Sci. USSR, 7(1965) 196
7. S.S. Batsanov and A.A. Deribas, Combustion, Explosion Shock Waves, 1(1965) 77
8. R.A. Graham et al., Annu. Rev. Mater. Sci., 16(1986) 315
9. Y. Horie, in J.R. Asay et al. (eds.), Shock Waves in Cond. Matter, (Elsevier, 1984), 369
10. Y.Horie, R.A. Graham and I.K. Simonsen, Mater. Lett., 3(1985) 354
11. R.A. Graham, Solids Under High-Pressure Shock Compression, Springer, New York, 1993
12. B. Krueger, A. Mutz and T. Vreeland Jr, Metall. Trans. 23A, 55(1991)

13. Y.Horie and M.E. Kipp, J. Appl. Phys., 63(1988) 5718
14. Y. Horie and A.B. Sawaoka, Shock Compression Chemistry of Materials, (Japan: KTK Scientific Publ.), 1993
15. M.B. Boslough, J. Chem. Phys., 92(3)(1990) 1839
16. N.N. Thadhani, Prog. Mater. Sci., 37(1992) 117
17. N.N. Thadhani, J. Appl. Phys., 76(1994) 2129
18. L.H. Yu and M.A. Meyers, J. Mater. Sci., 26(1991) 601
19. L.H. Yu and M.A. Meyers, in M.A. Meyers, L.E. Murr and K.P. Staudhammer (eds.), Shock-Wave and High-Strain-Rate Phenomena in Materials, (New York, NY:M. Dekker, Inc, 1992) 303
20. P.W. Bridgman, Phys. Rev. 48(1935) 825
21. M.A. Lange and T.J. Ahrens, J. Earth Plan Sci. Lett., 77(1986) 409
22. L.H. Yu, Ph.D. Thesis, New Mexico Institute of Mining and Technology
23. L.H. Yu, W. Nellis, M.A. Meyers and K.S. Vecchio, in S.C. Schmidt, J.W. Shaner, G.A. Samara and M. Ross(eds.), Shock Compression of Condensed Matter-1993, Am. Inst. Physics (1994) 1291
24. V.F. Nesterenko et al., Appl. Phys. Lett., 65(24)(1994), 3069
25. M.A. Meyers et al., Mater. Sci. and Eng., 201A(1995) 150
26. M.A. Meyers, L.H. Yu and K.S. Vecchio, Acta Metall. Mater., 42(3), (1994) 715
27. L.H. Yu and M.A. Meyers, J. Matls. Sci., 26(1991) 601
28. B.R. Krueger and T. Vreeland, Jr., J. Appl. Phys., 69(2), (1991) 710
29. K.S. Vecchio, L.H. Yu and M.A. Meyers, Acta Metall. Mater., 42(3), (1994) 701
30. F.R. Norwood and R.A. Graham, in Shock-Wave and High-Strain-Rate Phenomena in Materials (edited by M.A. Meyers, L.E. Murr and K.P. Staudhammer, New York, NY:Marcel Dekker, Inc), (1992) 989
31. S.S. Batsanov, "Effect of Explosions on Materials", (New York, NY: Springer, 1994)
32. R. Prummer, Explosivverdichtung Pulvriger Substanzen, (Berlin: Springer, 1982)
33. M.A. Meyers and S.L Wang, Acta Metall., 36(1988) 925
34. J. Reaugh, J. Appl. Phys., 61(3)(1987) 962
35. V.F. Nesterenko, M.P. Bondar and I.V. Ershov, in "High-Pressure Science and Technology - 993", (edited by S.C. Schmidt, J.W. Shaner, G.A. Samara and M. Ross, New York: Am. Inst. Phys., 1994) 1172
36. V.F. Nesterenko, A.N. Lazaridi and S.A. Pershin, Fiz. Goreniyz Vzryva, 25(1989) 154
37. C.J. Shih and V.F. Nesterenko and M.A. Meyers, 'High-strain-rate deformation and comminution of silicon carbide', J. of Applied Physics, 83(9), (1998) 4660
38. H.C. Chen, V.F. Nesterenko and M.A. Meyers, "Shear Localization and Chemical Reaction in High-Strain Rate Deformation of Ti-Si Powder Mixtures", in press, Acta Material (1998)
39. N.N. Thadhani et al., J. Appl. Phys., 82(1997) 1113-1128
40. A. Ferreira et al., Met. Trans., 22A (1991) 685
41. G. Johnson and W. Cook, Proc. 7th Int. Symp. Ballistics, Hague, Netherlands, (1983) 955
42. H.C. Chen, V.F. Nesterenko and M.A. Meyers,"Shear Localization and Chemical Reaction in Ti-Si and Nb-Si Powder Mixtures: Thermochemical Analysis", J. Appl. Physics, in press (1998)